*Proc. International Conference on Mechanical, Automotive and Mechatronics Engineering (ICMAME 2023)*
*29-30 April 2023, Dubai, UAE*

# Thermal Management for Zero-Gravity Applications using PCM-based Plate-Fin Heatsink

Mohammed Azzam
*Department of Mechanical Engineering*
*American University of Sharjah*
Sharjah, UAE
b00049820@alumni.aus.edu

Mohammad O. Hamdan
*Department of Mechanical Engineering*
*American University of Sharjah*
Sharjah, UAE
mhamdan@aus.edu

Maen Alkhader
*Department of Mechanical Engineering*
*American University of Sharjah*
Sharjah, UAE
malkhader@aus.edu

Frank Gerner
*Department of Mechanical and Materials Engineering*
*University of Cincinnati*
Cincinnati, USA
frank.gerner@uc.edu

***Abstract*— In this study, we numerically investigated the heat removal effectiveness of various phase change materials (PCMs) when injected into a plate-fin heatsink with a fixed thermal conductivity enhancer (TCE) volume fraction of 9%. This study focuses on examining the effects of fin numbers and PCM types. The numerical simulation, using ANSYS commercial software, shows that the performance of the PCM-infused heatsink has improved as the number of fins increases. When a plate-fin heatsink soaked in paraffin wax and exposed to a heat-flow density of 4 kW/m$^2$ for 30 minutes, the maximum temperature did not exceed 70°C for the 4-fin design but it exceeded 80°C for the 0- and 2-fin design. The salt hydrate PCM has shown superior performance when compared to paraffin wax and RT35. The zero-fin model has taken double the time required to melt all the PCM when compared to 2- and 4- fin heatsinks.**

***Keywords*— Melting and solidification, phase change material, electronics thermal management, plate-fin heatsink.***

## I. INTRODUCTION

The lifecycle and performance of electronic devices depends on the effectiveness of heat removal from these devices. Electronics equipment's needs to operate at temperature below the maximum allowed temperature otherwise their performance could lag during both steady-state and transient operations. Hence, different electronics cooling techniques have been developed such as heatsinks, fans, jet impingement [1, 2], heat pipes, loop heat pipes [3], porous media [4], micro-channel liquid cooling and phase change materials (PCMs). These cooling methods can be divided into passive cooling, which usually used for low heat-flow density applications and active cooling which usually used for high flux application. Active cooling requires power to operate and is used for high heat-flow density applications, while passive cooling does not require external power to operate and is used for low heat flux applications [5].

Phase change materials are reliable thermal management techniques that have been proposed for transient electronics operation. Due to its high latent specific heat capacity, PCMs use a passive cooling strategy and are capable of dissipating substantial amounts of thermal energy. PCMs are able to keep the temperature below the maximum permitted temperature for electronics that work for brief periods of time, like electric switches, or operate in an adiabatic environment, like rockets. In order for a PCM-infused heatsink to function effectively, all of the PCM must melt before the electronic gadget reaches its maximum allowable temperature [5].

The physical characteristics of a PCM, particularly its thermal conductivity, specific heat capacity, melting temperature, latent heat of fusion, and liquid phase viscosity, determine how well it can dissipate heat. Numerous studies have been conducted on synthesizing PCMs with elevated thermal conductivity, superior latent heat of fusion, improved specific heat capacity, high specific melting temperature, and low liquid phase viscosity. These studies have focused on enhancing the effectiveness of heat removal of the PCM-infused heatsink by adding thermally conductive enhancer such as fins, nanoparticles, and porous inserts.

Examining PCMs using numerical techniques present different challenges such involvements of Multiphysics phenomena (such as mass transfer, phase change, conduction and convection heat transfer), drastic variations in characteristics with temperature (due to volume expansion and buoyancy forces) and defining the size and structure of the PCM mushy zone.

Accurate numerical modelling of these phenomena is difficult and often requires experimental studies [6]. The difficulties in modelling PCMs include the lack of availability of properties as function of temperature, namely, volume expansion, thermal conductivity, and mushy zone size. Nevertheless, numerical models offer an opportunity to improve the design of PCM-heatsinks design by providing quantitative thermal improvements. Numerical studies can investigate the effect of various design parameters on heatsink performance. Arshad et al. [7] numerically tested the effect of fin thickness on PCM-heatsinks design and showed that melting time increases as heat load. decreases. The impact of paraffin wax infused in aluminum structure was investigated numerically [8], who showed that the effect of forced convection is directly influenced by fin structure, alignment with gravity, and fin volume fraction. Alazwari et al. [9] reported that adding carbon nanoparticles has improved the performance PCM energy storage while adding metal nanoparticles has hindered its performance. Arshad et al. [10] reported that adding copper nanoparticles with 0.01 volume

fraction has improved the performance by 2%, whereas heat storage capacity density was dropped by 7%. The numerical work by Qureshi et al. [11] has showed that triply periodic minimal surfaces foam outperformed conventional metal foam., Infusing PCM in a copper porous mesh has enhanced PCM performance under intermittent operations [12]. Many PCMs are widely used in commercial applications or researched for optimization, such as paraffin wax, n-Eicosane and Gallium. A study by Hasan et al. [13] have shown that milk fat is less effective than salt hydrate and paraffin wax, and milkfat.

The current study focuses on determining the main factors affecting the performance of a plate-fin heatsink when it is infused with a PCM under zero gravity. A 2D numerical simulation is constructed to examine the effect of different parameter, mainly, number of fins, types of PCM and heat-flow density rate. The problem is modelled using ANSYS-Fluent commercial software. The model is used to calculate expected time for PCM to melt for different heatsinks.

Electronics cooling is essential for maintaining the reliability and longevity of electronic devices. The electronics cooling is needed to remove the heat generation in the electronics which can damage the device or cause it to malfunction. Cooling systems help to dissipate the heat generated by electronic components and prevent them from overheating. This improve the electronics performance. Cooling systems help to maintain the optimal operating temperature of electronic devices, which can improve their performance and prevent issues like data loss or corruption. Also, it improves the lifespan of electronics components. This, also, reduce the risk of fire in these components. In some cases, overheating can pose a safety risk. For example, batteries that overheat can explode or catch fire.

## II. MATHEMATICAL AND NUMERICAL FORMULATION

The current problem schematic is shown in Figure 1 where a symmetric half domain is used to reduce computation time. Fig. 1a shows zero plate-fin heatsink, Fig. 1b shows a two plate-fin heatsink and Fig. 1c shows a four plate-fin heatsink. The three heatsink models are examined under heat load of namely, $4{,}000\ W/m^2$. All heat sinks have the height of 17 mm and a square base with width length of 85 mm. The constant heat flux area is square with width o 50 mm. The base of the heatsink has was thickness of 3 mm.

A transient analysis is conducted with an initial temperature of the full computational region set to 290 K. The flow is assumed laminar incompressible Newtonian viscous flow and all properties are assumed isotropic and constant. The value of the thermal physical properties used in this numerical study is shown in Table 1.

The PCM is assumed perfect incompressible material with same density value for liquid and solid. A uniform and steady state heat-flow density is applied at the bottom plate of the heatsink and is operated for a duration of 30 minutes after which it is turned off. The heatsink is placed in area with force convection heat transfer coefficient of $30\ \mathrm{W/(m^2.°C)}$ and temperature of 290K. The density of liquid is assumed equal the density of solid state which greatly simplify the problem where the PCM volume is assumed stay constant during melting. A fixed TCE volume fraction of 9% is employed in this study which directly impacted the fin thickness for case of 2- and 4- fin heatsink designs.

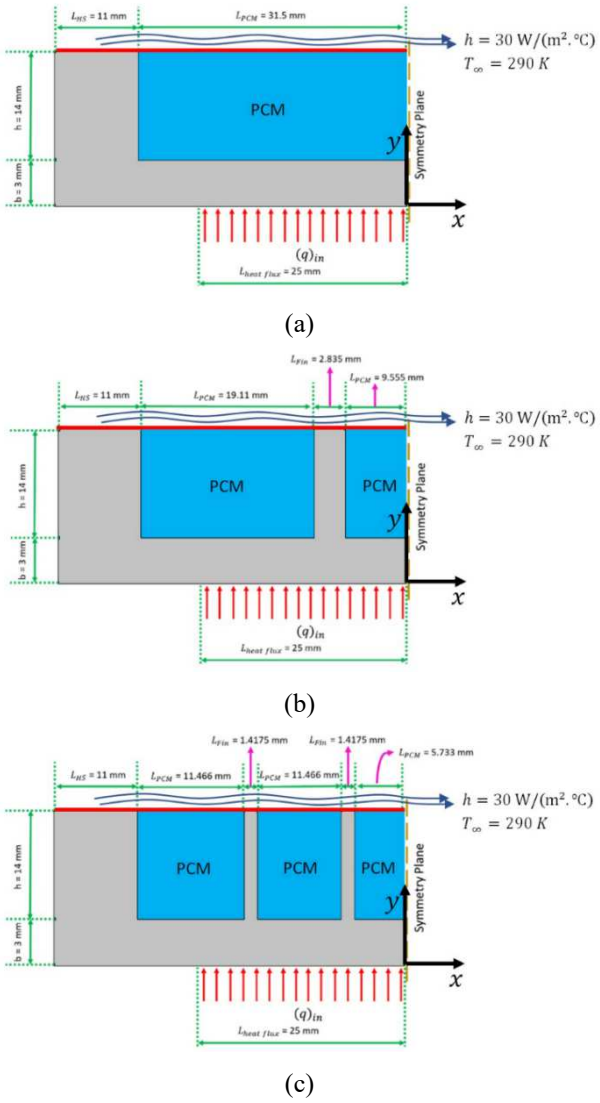


Fig. 1. A schematic diagram of three different heatsink models, namely (a) zero-plate-fin, (b) 2-plate-fin, and (c) 4-plate-fin.

TABLE I. THERMAL PHYSICAL PROPERTIES OF DIFFERENT MATERIAL USED IN THIS NUMERICAL SIMULATION

| Material properties | Salt hydrate [14] | Paraffin wax [15] | RT35 [16] | Aluminum |
|---|---|---|---|---|
| Thermal conductivity $[\mathbf{W/(m.K)}]$ | 0.6 | 0.2 | 0.2 | 202.37 |
| Specific heat capacity $[\mathbf{kJ/(kg.K)}]$ | 2 | 2.2 | 2 | 0.871 |
| Density $[\mathbf{kg/m^3}]$ | 1,500 | 802 | 780 | 2719 |
| Dynamic Viscosity $[\mathbf{kg/(m.s)}]$ | 0.00184 | 0.003 | 0.0247 | - |
| Solidus temperature [°C] | 27 | 37.53 | 34 | - |
| Liquidus temperature [°C] | 32 | 42.89 | 35 | - |
| Latent heat of fusion [kJ/kg] | 200 | 141.7 | 160 | - |

The TCE volume fraction is defined as follow:

$$\psi_{TCE} = \frac{\text{Volume of Fins}}{\text{Volume of Fins and gaps between fins}} \quad (1)$$

The fin thickness for the case of 2- and 4- fin designs have been calculated by employing a TCE volume fraction of 9%. Based on the assumptions introduced earlier, the heatsink with PCM can modeled using the following equations:

The continuity equation in the liquid PCM

$$\vec{\nabla} \cdot \vec{u} = 0 \quad (2)$$

The momentum equations in the liquid PCM

$$\frac{\partial(\rho_l \vec{u})}{\partial t} + (\vec{u} \cdot \vec{\nabla})\rho_l \vec{u} = -\vec{\nabla} p + \mu_l \nabla^2 \vec{u} + \rho_l \vec{g} \beta (T - T_{ref}) - A\,\vec{u} \quad (3)$$

The region between liquid phase and solid phase in PCM is known by the "mushy zone" which is modelled using the porosity function ($A$) shown in equation (4). The "mushy zone" is modelled, as suggested in literature, as a porous region using a modified form of the Carmane-Kozeny equations, where $A$ is defined as follow [17]:

$$A = \frac{C(1-f_l)^2}{\varepsilon + f_l^3} \quad (4)$$

Where $\varepsilon$ is a small arbitrary constant (=0.001), and $C$ is a mushy zone damping amplitude of liquid PCM velocity when passing through the mushy zone. The parameter ($f_l$) represents the liquid fraction of PCM, which define as follow:

$$f_l = \begin{cases} 0 & if \quad T < T_{Solidus} \\ \left(\frac{T - T_{Solidus}}{T_{Liquidus} - T_{Solidus}}\right) & if \quad T_{Solidus} < T < T_{Liquidus} \\ 1 & if \quad T > T_{Liquidus} \end{cases} \quad (5)$$

The transient conservation energy equation in the liquid PCM is shown below:

$$\rho_l c_{p,l} \frac{\partial T}{\partial t} + \rho_l c_{p,l}\, \vec{u} \cdot \vec{\nabla} T = \vec{\nabla} \cdot (k_l \vec{\nabla} T) - \rho_l L \frac{\partial f_l}{\partial t} \quad (6)$$

The last term in the energy equation of the liquid PCM represents the amount of heat absorbed when solid changes phase to liquid, where $L$ is the latent heat of fusion.

The transient conservation energy equation in the solid PCM and solid heatsink are shown below, respectively:

$$\rho_s c_{p,s} \frac{\partial T}{\partial t} = \vec{\nabla} \cdot (k_s \vec{\nabla} T) \quad (7)$$

$$\rho_{HS} c_{p,HS} \frac{\partial T}{\partial t} = \vec{\nabla} \cdot (k_{HS} \vec{\nabla} T) \quad (8)$$

## III. 3. Numerical Formulation

A commercial CFD tool, ANSYS-Fluent, is used to solve the present problem numerically with a transient pressure-based solver. Mesh independence study, shown in Figure 2, has been conducted to assure that proper mesh is used and that results do not depend on mesh size. For more details on the mesh study, the reader is advised to visit the work done by Azzam et al. [18]. The spatial discretization performed in this study is cell-based least-squares for gradient, quadratic for pressure, and downwind quadratic for momentum and energy. Residuals introduced for continuity and velocity are set to $1 \times 10^{-6}$, while the residual for the energy is set to $1 \times 10^{-13}$. An adaptive time solution is used to reduce the possibility of time step accumulation errors during computation. The time progression method is set to error-based instead of CFL-based. The physical time for this issue is set to 30 minutes, the time error tolerance is set to 0.01, the initial time step size is set to 0.01 seconds and the maximum time step size to 10 seconds. The small-time step is used to properly capture the transient behavior in the beginning of the process where change is fast, while the large time step is used to speed the process when changes are slow. The maximum number of iterations is set to 100 for each time step, allowing the solver to converge at any time step size. Convergence is achieved for all iterations and models.

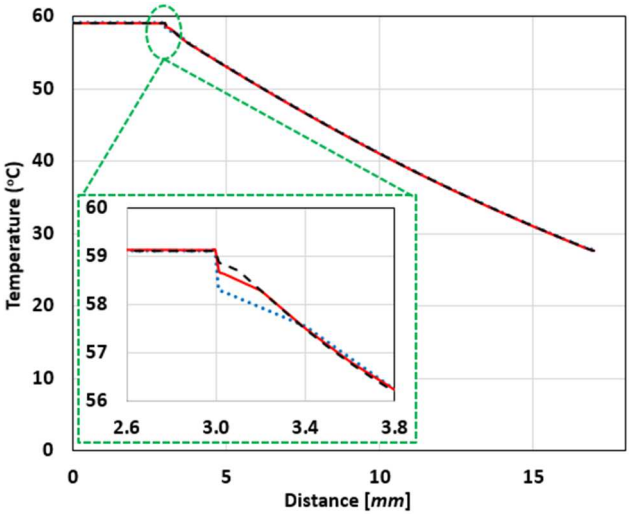


Fig. 2. Mesh independent study.

## IV. Results and Discussion

The results show how various heatsink factors, primarily (1) fin count and (2) PCM type, affect performance of plate-fin heatsink infused with PCM. Both the time needed for the PCM to fully melt and the time needed for it to solidify are reported in the study.

The amount of heat removed from the heatsink for different number of fins is shown in Figures 3. The temperature profiles are plotted for the three heatsink models when infused with paraffin wax at a time of 30 minutes under a heat-flow density of 4 kW/m$^2$. The heat is transferred from the heatsink bottom toward the top, where it leaves by forced convection. Therefore, the temperature decreases toward the top side of the heatsink, as shown in Figure 3. The 4-fin heatsink produces the lowest temperature rise across the line of symmetry, and the lowest maximum temperature. The 4-fin heatsink model has better conduction when compared to the other heatsink models. The better effective thermal conductance of the 4-fin heatsink increases the heat transfer which permits more effective use of the PCM. As the PCM absorbs more heat, one would expect lower temperatures. Hence, the lowest maximum temperature is attained using a 4-fin, then a 2-fin, followed by the zero-fin heatsink. The temperature is almost uniform across the first 3 mm of the heatsink which represents the thickness of the bottom plate.

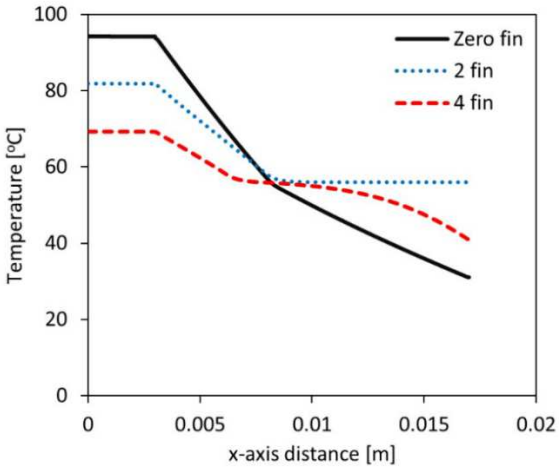


Fig. 3. Temperature profiles along the symmetry line of a heatsink infused with paraffin wax with heat-flow density of 4 $kW/m^2$ at time of 30 minutes.

Figure 4 shows the midpoint transient temperature when using paraffin wax with a heat-flow density of 4 $kW/m^2$. As discussed earlier, the 4-fin heatsink provides better heat transfer to the top surface as compared to other heatsink designs. The ability of the fins to move the heat toward the top side of the heatsink provides better heat dissipation and increases the time needed to reach the maximum permissible operating temperature of 100°C. As shown in Figure 4, for a heat-flow density of 4 $kW/m^2$, none of the heatsink models reach the maximum permissible temperature. The Figure shows that after 30 minutes of operation, the zero-fin, 2-fin and 4-fin heatsink reach temperature of 94 ℃, 82 ℃ and 70 ℃, respectively.

Figure 5 shows the effect of the type of PCM (paraffin wax, salt hydrate and RT35) infused inside a 4-fin heatsink. These temperature profiles are plotted the three PCMs at 30 minutes and under a heat-flow density of 4 $kW/m^2$. The figure shows that salt hydrate is the best performer compared to the other PCM's, followed by paraffin wax and lastly by RT35. This behavior is mainly dependent on the thermal properties and phase status of these PCM's.

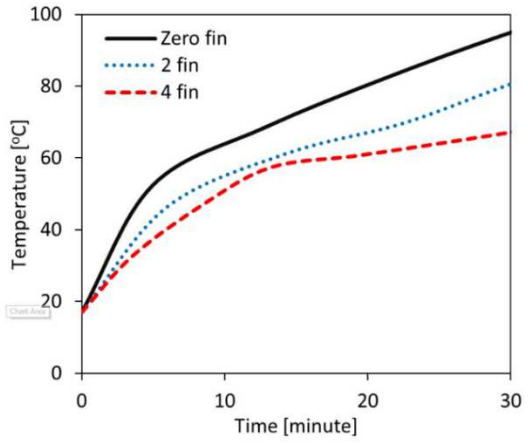


Fig. 4. The temperature variation of midpoint with time for all heatsink models when infused with paraffin wax under heat-flow density of 4 $kW/m^2$

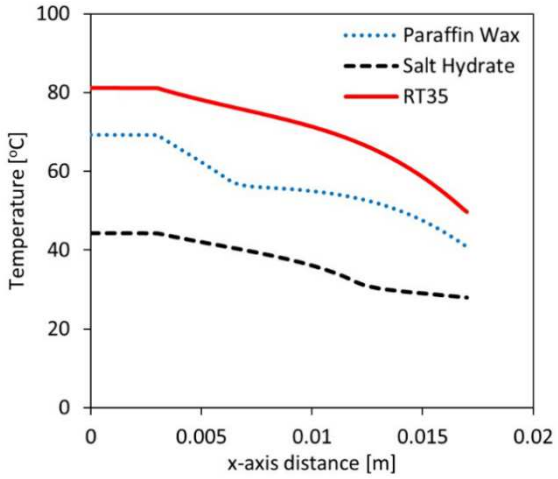


Fig. 5. Temperature profiles along the symmetry line of a 4 plate-fin heatsink model infused with different PCMs with heat-flow density of 4 $kW/m^2$ at time of 30 minutes.

Figure 6 shows the midpoint transient temperature for 4-fin heatsink under heat-flow density of 4 $kW/m^2$. As seen in Figure 6, all three PCMs start at the same initial temperature. From figure 5, RT35 outperforms paraffin wax in the time range 7-20 minute, but paraffin wax outperforms RT35 when most of RT35 becomes liquid. This behavior depends on how long it takes for the PCM to fully melt. As seen in Figure 5, we can see that the temperature rises sharply at first and then drops as melting begins. Therefore, RT35 begins to melt first, followed by the salt hydrate, followed by the paraffin wax. Salt hydrate work best with 30 minutes of operation under the given conditions.

Quantifying how long it takes to melt all the PCM is important for choosing the best PCM for a specific application. Figure 7 shows the time it takes for the entire PCM domain to melt for various heatsink models. For the same PCM, the zero fin heatsink model takes the longest compared to the other heatsink models. The time required to completely melt the PCM depends on how fast heat is being removed from the heat source to the surrounding. The heat removal is improved by the addition of fins and heat removal is higher in PCM with higher thermal conductivity. RT35 is the first PCM to melt, followed by salt hydrate and paraffin wax. Salts hydrate have higher latent heats and densities than paraffin waxes, but do not have the longest melting times. This is because salt hydrate has three times the thermal conductivity of paraffin wax, improving heat transfer through the heatsink matrix.

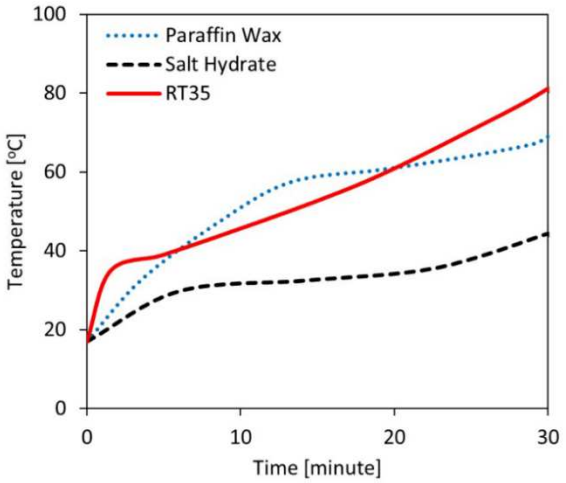


Fig. 6. The variation of midpoint temperature with time for the 4-fin heatsink model when infused with three different PCM's under a heat-flow density of 4 $kW/m^2$.

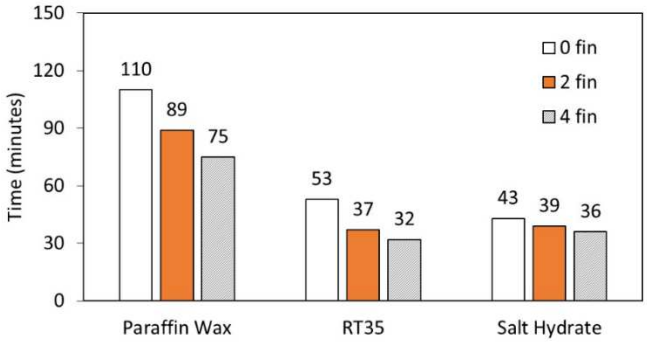


Fig. 7. The time required for all the PCM to phase change from solid state to liquid state under heat-flow density of 4 $kW/m^2$.

## V. Conclusions

The study has numerically examined the performance of various PCM impregnated in three heatsink designs, mainly zero-fin, two-fin, and four-fin heatsinks. A parametric study is performed to optimize the design with different number of fin and different PCMs. The three PCMs used in this study are paraffin wax, RT35, and salt hydrate. The results show that increasing the number of fins improves the performance of the PCM-heatsink system. The zero-fin heatsink took the longest to time to completely melt all the PCM in the heatsink compared to the 2-fin and 4-fin heatsink design due to the additional amount of PCM present in the heatsink area. Comparing different PCMs, salt hydrate outperforms paraffin wax and RT35, with paraffin wax taking the longest to completely dissolve all PCMs. The study shows that it is recommended to use salt hydrate and 4-fin heat sink to achieve desired transient cooling.

## Acknowledgements

The authors recognize the American University of Sharjah support for this study. This work was partially supported by the Mechanical Department at the American University of Sharjah and research fund number FRG20-M-E32. This paper represents the opinion of the author and does not represent the position or opinion of the institute.

## References

[1] M. Al-Hemyari, M. O. Hamdan, and M. F. Orhan, "Optimization of a confined jet geometry to improve film cooling performance using response surface methodology (RSM)," *Processes,* vol. 8, p. 232, 2020.

[2] M. Al-Hemyari, M. O. Hamdan, and M. F. Orhan, "A numerical analysis of the slot film-cooling effectiveness," in *2018 Advances in Science and Engineering Technology International Conferences (ASET)*, 2018, pp. 1-7.

[3] D. Cytrynowicz, M. Hamdan, P. Medis, H. T. Henderson, and F. M. Gerner, "Test cell for a novel planar MEMS loop heat pipe based on coherent porous silicon," in *AIP Conference Proceedings*, 2003, pp. 227-238.

[4] M. Hamdan and M. d. A. Al-Nimr, "The use of porous fins for heat transfer augmentation in parallel-plate channels," *Transport in porous media,* vol. 84, pp. 409-420, 2010.

[5] B. Ding, W.-C. Feng, J. Fang, S.-Z. Li, and L. Gong, "How natural convection affect cooling performance of PCM heat sink," *International Journal of Heat and Mass Transfer,* vol. 184, p. 122272, 2022.

[6] N. S. Bondareva and M. A. Sheremet, "Influence of PCM heat sink shape on cooling of heat-generating elements in electronics," *Applied Thermal Engineering,* p. 118695, 2022.

[7] A. Arshad, M. Jabbal, P. T. Sardari, M. A. Bashir, H. Faraji, and Y. Yan, "Transient simulation of finned heat sinks embedded with PCM for electronics cooling," *Thermal Science and Engineering Progress,* vol. 18, p. 100520, 2020.

[8] J. Xie, K. F. Choo, J. Xiang, and H. M. Lee, "Characterization of natural convection in a PCM-based heat sink with novel conductive structures," *International Communications in Heat and Mass Transfer,* vol. 108, p. 104306, 2019.

[9] M. A. Alazwari, M. Algarni, and M. R. Safaei, "Effects of various types of nanomaterials on PCM melting process in a thermal energy storage system for solar cooling application using CFD and MCMC methods," *International Journal of Heat and Mass Transfer,* vol. 195, p. 123204, 2022.

[10] A. Arshad, M. Jabbal, H. Faraji, P. Talebizadehsardari, M. A. Bashir, and Y. Yan, "Numerical study of nanocomposite phase change material-based heat sink for the passive cooling of electronic components," *Heat and Mass Transfer,* pp. 1-15, 2021.

[11] Z. A. Qureshi, E. Elnajjar, O. Al-Ketan, R. A. Al-Rub, and S. B. Al-Omari, "Heat transfer performance of a finned metal foam-phase change material (FMF-PCM) system incorporating triply periodic minimal surfaces (TPMS)," *International Journal of Heat and Mass Transfer,* vol. 170, p. 121001, 2021.

[12] Q. Ren, Z. Wang, J. Zhu, and Z. Qu, "Pore-scale heat transfer of heat sink filled with stacked 2D metal fiber-PCM composite," *International Journal of Thermal Sciences,* vol. 161, p. 106739, 2021.

[13] A. Hasan, H. Hejase, S. Abdelbaqi, A. Assi, and M. O. Hamdan, "Comparative effectiveness of different phase change materials to improve cooling performance of heat sinks for electronic devices," *Applied Sciences,* vol. 6, p. 226, 2016.

[14] I. Mjallal, H. Farhat, M. Hammoud, S. Ali, and I. Assi, "Improving the cooling efficiency of heat sinks through the use of different types of phase change materials," *Technologies,* vol. 6, p. 5, 2018.

[15] W. A. Dukhan, N. S. Dhaidan, and T. A. Al-Hattab, "Experimental investigation of the horizontal double pipe heat exchanger utilized phase change material," in *IOP Conference Series: Materials Science and Engineering*, 2020, p. 012148.

[16] V. Nandana and U. Janoske, "Experimental and numerical study on the melting behaviour of a phase change material in buoyancy driven flows," in *7th European Conference on Computational Fluid Dynamics*, 2018.

[17] V. R. Voller and C. Prakash, "A fixed grid numerical modelling methodology for convection-diffusion mushy region phase-change problems," *International journal of heat and mass transfer,* vol. 30, pp. 1709-1719, 1987.

[18] M. Azzam, M. Hamdan, M. Alkhader, and F. M. Gerner, "Analysis of Plate-Fin Heat Sink Infused with Phase Change Materials for Intermittent Space Missions," *Journal of Enhanced Heat Transfer,* 2023.